Journal of Cellular Biochemistry

# SIRT3 silencing sensitizes breast cancer cells to cytotoxic treatments through an increment in ROS production

| | |
|---|---|
| Journal: | *Journal of Cellular Biochemistry* |
| Manuscript ID | JCB-16-0253.R1 |
| Wiley - Manuscript type: | Research Article |
| Date Submitted by the Author: | n/a |
| Complete List of Authors: | Torrens-Mas, Margalida; Grupo multidisciplinar de Oncología Traslacional, Institut Universitari d'Investigació en Ciències de la Salut ; Fisiopatología Obesidad y Nutrición (CB06/03), Instituto de Salud Carlos III; Instituto de Investigación Sanitaria de Palma (IdISPa), Hospital Universitario Son Espases, edificio S<br>Pons, Daniel Gabriel; Grupo multidisciplinar de Oncología Traslacional, Institut Universitari d'Investigació en Ciències de la Salut ; Fisiopatología Obesidad y Nutrición (CB06/03), Instituto de Salud Carlos III; Instituto de Investigación Sanitaria de Palma (IdISPa), Hospital Universitario Son Espases, edificio S<br>Sastre-Serra, Jorge; Grupo multidisciplinar de Oncología Traslacional, Institut Universitari d'Investigació en Ciències de la Salut ; Fisiopatología Obesidad y Nutrición (CB06/03), Instituto de Salud Carlos III; Instituto de Investigación Sanitaria de Palma (IdISPa), Hospital Universitario Son Espases, edificio S<br>Oliver, Jordi; Grupo multidisciplinar de Oncología Traslacional, Institut Universitari d'Investigació en Ciències de la Salut , Fundamental Biology and Health Science; Fisiopatología Obesidad y Nutrición (CB06/03), Instituto de Salud Carlos III, ; Instituto de Investigación Sanitaria de Palma (IdISPa), Hospital Universitario Son Espases, edificio S.<br>Roca, Pilar; Grupo multidisciplinar de Oncología Traslacional, Institut Universitari d'Investigació en Ciències de la Salut , Fundamental Biology and Health Science; Fisiopatología Obesidad y Nutrición (CB06/03), Instituto de Salud Carlos III, ; Instituto de Investigación Sanitaria de Palma (IdISPa), Hospital Universitario Son Espases, edificio S. |
| Keywords: | Breast cancer, SIRT3, Oxidative stress, Tamoxifen, Cisplatin |
| | |

**TITLE PAGE**

# SIRT3 silencing sensitizes breast cancer cells to cytotoxic treatments through an increment in ROS production

**Authors names and affiliations:**
Margalida Torrens-Mas, Daniel Gabriel Pons, Jorge Sastre-Serra, Jordi Oliver*, Pilar Roca

Grupo Multidisciplinar de Oncología Traslacional, Institut Universitari d´Investigació en Ciències de la Salut (IUNICS), Palma de Mallorca, Illes Balears, Spain.
Ciber Fisiopatología Obesidad y Nutrición (CB06/03) Instituto Salud Carlos III, Madrid, Spain.
Instituto de Investigación Sanitaria de Palma (IdISPa), Hospital Universitario Son Espases, edificio S. E-07120 Palma de Mallorca, Illes Balears, Spain.

*** Corresponding author:**
Dr. Jordi Oliver. *Departamento de Biología Fundamental y Ciencias de la Salud. Universitat de les Illes Balears. Cra de Valldemossa, km 7'5.07122 Palma de Mallorca, España. Tel*: (+34) 971259643; *Fax: (+34) 971 173184; e-mail: jordi.oliver@uib.es*

**Keywords:**

- **Breast cancer**
- **SIRT3**
- **Oxidative stress**
- **Tamoxifen**
- **Cisplatin**

**Total number of text figures**: 6

**Abstract**

SIRT3, the major deacetylase in mitochondria, plays a crucial role modulating ROS production and scavenging by regulating key proteins implicated in mitochondrial turnover and in antioxidant defenses. Therefore, SIRT3 could confer resistance to chemotherapy-induced oxidative stress, leading to a lower ROS production and a higher cell survival. Our aim was to analyze whether SIRT3 silencing in breast cancer cells through a specific siRNA could increase oxidative stress and thus compromise the antioxidant response, resulting in a sensitization of the cells to cisplatin (CDDP) or tamoxifen (TAM). For this purpose, we studied cell viability, ROS production, apoptosis and autophagy in MCF-7 and T47D cell lines treated with these cytotoxic compounds, these either alone, or in combination with SIRT3 silencing. Moreover, protein levels regulated by SIRT3 were also examined and survival curves were analyzed to study the importance of SIRT3 expression for the overall survival of breast cancer patients. When SIRT3 was silenced and combined with cytotoxic treatments, cell viability was highly decreased, and was accompanied by a significant increase in ROS production. While TAM treatment increased autophagic cell death, CDDP significantly triggered apoptosis, whereas SIRT3 silencing produced an enhancement of these two action mechanisms. SIRT3 knockdown also affected PGC-1α and TFAM (mitochondrial biogenesis), and MnSOD and $IDH_2$ (antioxidant defenses) protein levels. Finally, survival curves showed that higher SIRT3 expression is correlated to a poorer prognosis for patients with grade 3 breast cancer. In conclusion, SIRT3 could be a therapeutic target for breast cancer, improving the effectiveness of CDDP and TAM treatments.

## Introduction

Breast cancer is the most frequently diagnosed malignancy and a leading cause of death among women worldwide, and represented 25% of all female cancers in 2012 (Ferlay et al., 2013; Youlden et al., 2012). Although estrogen exposure constitutes a well-known risk factor for developing breast cancer (Chen et al., 2008), previous studies have pointed out that reactive oxygen species (ROS) and an altered mitochondrial function may have key roles in the progression of this disease (Roca et al., 2014).

Mitochondria are the major source of ROS in the cell because of the metabolic reactions that take place in these organelles. High levels of ROS can lead to oxidative stress, cause damage to proteins, lipids, and DNA, as well as contribute to genomic instability and tumor promotion (Finley and Haigis, 2012; Valle and Roca, 2012). Furthermore, when ROS levels rise above a certain threshold, which is at a higher level in cancer cells than in normal ones, ROS can induce apoptosis and cellular senescence (Sainz et al., 2012; Valle and Roca, 2012). This situation occurs with the use of some of the current anticancer therapies, such as cisplatin (CDDP) and tamoxifen (TAM). CDDP forms DNA adducts and is used against a wide variety of tumors (Kelland, 2007; Siddik, 2003), while TAM inhibits the estrogen receptor alpha (ER-α) and induces cell arrest, which is why this latter therapy is the main choice of treatment for ER-positive breast tumors (Razandi et al., 2013; Zhang et al., 2013). However, both CDDP and TAM alter mitochondrial function and contribute to increase oxidative stress in cancer cells (Pons et al., 2015a; Zhang et al., 2013).

Recent studies suggest that sirtuin 3 (SIRT3), a member of a family of $NAD^+$-dependent deacetylases, is implicated in the oxidative stress response through the regulation of mitochondrial metabolism and antioxidant mechanisms (Alhazzazi et al., 2013; Finley and Haigis, 2012; Papa and Germain, 2014). SIRT3 enters the mitochondria to ameliorate oxidative stress by deacetylation of its targets, such as: oxidative phosphorylation complexes (OXPHOS) subunits, manganese superoxide dismutase (MnSOD), isocitrate dehydrogenase ($IDH_2$) or glutamate dehydrogenase (Bause and Haigis, 2013; Finley and Haigis, 2012; Sack and Finkel, 2012; Weir et al.,

2013; Zhu et al., 2014). Thus, SIRT3 is a protection mechanism in normal cells; however, its activity could also protect cancer cells from chemotherapy-induced oxidative stress. In fact, tamoxifen induced overexpression of SIRT3 in breast cancer cells, which in turn conferred resistance to these cells for the treatment (Papa and Germain, 2014; Zhang et al., 2013). Different studies have also found a significant correlation between SIRT3 levels and progression of several types of cancer, such as breast, colon or oral cancer (Chen et al., 2014; Desouki et al., 2014; He et al., 2014; Liu et al., 2014; Wei et al., 2013; Zhang et al., 2013).

Another important target of SIRT3 is forkhead box 3a (FOXO3a), a transcription factor that controls mitochondrial turnover through the regulation of processes such as mitochondrial biogenesis, mitochondrial dynamics and mitophagy (Tseng et al., 2013). Furthermore, FOXO3a upregulates antioxidant enzymes such as MnSOD, peroxiredoxin 3, and catalase in order to protect cells against oxidative stress (Bause and Haigis, 2013; Tseng et al., 2013). Thus, SIRT3 can indirectly affect expression levels of proteins related to mitochondrial homeostasis through deacetylation of FOXO3a.

The aim of this study was to analyze whether small interfering RNA siRNA-mediated SIRT3 silencing could increase oxidative stress and lead to mitochondrial dysfunction, and consequently make cancer cells more sensitive to cytotoxic treatments of breast cancer. For this purpose, we studied two human breast cancer cell lines, MCF-7 and T47D. Previous studies in our group showed that these lines exhibit different regulatory mechanisms for oxidative stress and treatment response (Nadal-Serrano et al., 2012; Sastre-Serra et al., 2012). Specifically, we silenced SIRT3 and treated cells with CDDP or TAM. Parameters such as ROS production, apoptosis, autophagy, and levels of different proteins were evaluated.

## MATERIALS AND METHODS

### *Reagents*

Dulbecco's Modified Eagle's medium (DMEM) high glucose was purchased from GIBCO (Paisley, UK). Cisplatin (*cis-diamminedichloroplatinum II or CDDP) and tamoxifen (trans-2-[4-(1,2-Diphenyl-1-butenyl)phenoxy]-N,N-dimethylethylamine or TAM)* were obtained from Sigma-Aldrich (St. Louis, MO, USA). Routine chemicals were supplied by Sigma-Aldrich (St. Louis, MO, USA), Roche (Barcelona, Spain), Panreac (Barcelona, Spain) and Bio-Rad Laboratories (Hercules, CA, USA).

### *Cell culture*

Human breast cancer cell lines MCF-7 and T47D were purchased from American Type Culture Collection (ATCC; Manassas, VA, USA) and maintained in DMEM supplemented with 10% (v/v) heat-inactivated fetal bovine serum (FBS) and 1% (v/v) antibiotics (penicillin and streptomycin) at 37 °C with 5% $CO_2$.

### *Cell transfection and treatments*

The day before transfection cells were plated in 6-well culture plates at a density of 3.5 x $10^5$ cells/well for Western Blot or in 96-well culture plates at a density of 1.5 x $10^4$ cells/well for cell viability and fluorometric assays. Transfection with a specific SIRT3 small interfering RNA (siRNA) was carried out with Lipofectamine 2000 reagent (Life Technologies, Thermo Fisher Scientific, Waltham, MA, USA) according to the manufacturer's protocol. After 6h of transfection, the siRNA-lipofectamine complexes were removed and cells were maintained in DMEM. The next day, cells were treated with 10 µM CDDP or 10 µM TAM for 48h using DMSO as a vehicle.

### *Cell viability assay*

Cells were transfected and treated as stated above. After treatment, cell viability was determined by crystal violet assay. Briefly, cells were stained with 0.5% (p/v) crystal violet in 30% (v/v) acetic acid for 10 min. After washing in distilled water, 100 µl of methanol were added to solubilize the dye and absorbance was measured *at* 595 nm using a PowerWave XS Microplate Spectrophotometer (BioTek Instruments, Inc.).

### *Colony formation assay*

To determine the cell survival rate after transfection and cytotoxic treatments, a clonogenic assay was performed as described before in Pons et al (2015a). Briefly, cells were trypsinized and seeded at low density, $5x10^3$ cells per 60-mm plate. Cells were cultured for up to 14 days and fresh culture medium was added three times per week. Colonies were stained with crystal violet and counted for each condition.

*Fluorometric measurement of ROS production*

To measure ROS production after treatment, the Amplex® Red Hydrogen Peroxide/Peroxidase Assay Kit (Molecular Probes, Eugene, Oregon, USA) was used. Briefly, 50 µM Amplex Red reagent and 0.1 U/ml horseradish peroxidase were diluted in Krebs-Ringer phosphate buffer and the reaction mixture was added to cells. Fluorescence measurement was recorded at times 0, 15, 30 and 60 minutes. An FLx800 microplate fluorescence reader (Bio-Tek Winooski, Vermont, USA) was used, set at excitation and emission wavelengths of 571 nm and 585 nm, respectively. Values were normalized per number of viable cells determined by crystal violet assay performed as described above.

*Fluorometric determination of autophagy*

Following treatment, autophagy was measured fluorimetrically using the Monodansyl cadaverine (MDC) probe as previously described by Dando et al (2013). Cells were stained with 50 µM MDC for 15 minutes and then rinsed with PBS. Fluorescence measurement was performed using an FLx800 microplate fluorescence reader (Bio-Tek Winooski, Vermont, USA). Excitation and emission wavelengths were set at 340 nm and 535 nm, respectively. All values were normalized per number of viable cells determined by crystal violet assay performed as described above.

*Apoptosis fluorometric assay*

Apoptosis was measured fluorometrically using Annexin V staining as described by Dando et al (2013). Briefly, after cytotoxic treatment, cells were fixed with 2% paraformaldehyde (BD Biosciences, NJ, USA) in PBS for 30 minutes at room temperature. After washing cells twice with PBS, Annexin V/AlexaFluor350 (Life Technologies, Thermo Fisher Scientific, Waltham, MA, USA) in annexin binding buffer (10 mM HEPES/NaOH pH 7.4, 140 mM NaOH and 2.5 mM $CaCl_2$) was added for 10 minutes in the dark at room temperature. Cells were rinsed twice with annexin binding buffer and fluorescence was measured. An FLx800 microplate fluorescence reader (Bio-Tek Winooski, Vermont, USA) was used and excitation and

emission wavelengths were set at 346 and 442 nm. Values were normalized per number of viable cells determined by crystal violet assay.

*Western blot analysis*

After treatment, cells were harvested by scraping them into 200 µL of RIPA buffer (50 mM Tris-HCl pH 7.5, 150 mM NaCl, 0.1% SDS, 0.5% deoxycholate, 1% Triton X-100, 1 mM EDTA, 0.01 mM leupeptin, 0.01 M pepstatin, 2 mM PMSF, 1 mM NaF and 1 mM $Na_3VO_4$) and disrupted by sonication at 40% amplitude for 10 seconds three times (VibraCell 75185). Samples were then centrifuged at 14000 ×*g* for 10 min at 4 °C and protein content (supernatant) was determined with a bicinchoninic acid (BCA) protein assay kit (Pierce, Bonn, Germany).

Twenty µg of protein from cell lysate were separated on 10% SDS–PAGE gels and electrotransferred to 0.22 µm or 0.45 µm nitrocellulose membranes (Bio-Rad). Membranes were blocked with 5% non-fat powdered milk in Tris-buffered saline-Tween (TBS with 0.05% Tween-20) for 1h. Antisera against SIRT3, PARP, LC3A/B, IDH, TFAM (Cell Signaling Technology Inc, Danvers, MA), PGC-1α (Abcam, Cambridge, UK), GAPDH and MnSOD (Santa Cruz Biotechnology, CA, USA) were used as primary antibodies. Protein bands were visualized by Immun-Star® Western C® Kit reagent (Bio-Rad) Western blotting detection systems. The chemiluminiscence signal was captured with a Chemidoc XRS densitometer (Bio-Rad) and results were analyzed with Quantity One Software (Bio-Rad).

*Immunoprecipitation and acetylation analysis*

After siRNA treatment for 72 hours, cells were harvested as described before for Western Blot analysis. Protein content was determined with a BCA protein assay and 1 µg of MnSOD antibody (Santa Cruz Biotechnology, CA, USA) was added to 200 µg of total protein to start immunoprecipitation. The mixture was kept rocking overnight at 4 °C. The next day, 7.5 µL of protein A-Agarose (Sigma-Aldrich, St. Louis, MO, USA) were added and the samples were incubated for 3h rocking at 4 °C and then centrifuged at 2500 *xg*, 4 °C for 30 seconds. Five washes with RIPA were made and the pellet was ressuspended in 15 µL of sample buffer. Samples were separated on 12% SDS-PAGE gels and electrotransferred to 0.22 µm nitrocellulose membrane, which was stained with Ponceau S and then rinsed with TBS-Tween. After blocking with 5% non-fat powdered milk in TBS-Tween, antiserum against acetylated-lysine (Cell signaling Technology Inc, Danvers, MA) was used as primary antibody. Protein bands were visualized by Immun-Star® Western C® Kit reagent (Bio-Rad) Western blotting

detection systems. The chemiluminiscence signal was captured with a Chemidoc XRS densitometer (Bio-Rad) and results were analyzed with Quantity One Software (Bio-Rad).

*Kaplan-Meier survival curves*

Kaplan-Meier plots were created using the online tool Kaplan-Meier plotter (www.kmplot.com) (Gyorffy et al., 2010). Overall survival (OS) was assessed for breast cancer patients. The mRNA JetSet best probe set for SIRT3 (221913_at) was used for the curves and the ER status was fixed as ER positive or ER negative, as checked by immunohistochemistry. Patients were split by median selecting the best cutoff and the follow up threshold was set to 5 years, censoring patients surviving over this threshold. For quality control, outlier arrays were excluded and redundant samples were removed. The analysis was performed including all grade 3 breast cancer patients and selecting the most recent update of the database (2014 version). These criteria allowed the analysis to run on 96 patients.

*Statistical analysis*

The Statistical Program for the Social Sciences software for Windows (SPSS, version 21.0; SPSS Inc, Chicago, IL) was used for all statistical analyses. Results are presented as mean values ± standard error of the mean (SEM). The effects of SIRT3 silencing and cytotoxic treatment were assessed using ANOVA, and Student's t-test was performed when there were combinatory effects. Statistical significance was set at $P<0.05$.

## RESULTS

*SIRT3 protein levels after siRNA transfection*

To ensure that SIRT3 was silenced after siRNA transfection, protein levels of SIRT3 were measured by Western blot (Representative bands are shown in Figure 1). SIRT3 levels decreased to 25% of control values in MCF-7 cells (A), while in T47D cells they were reduced by 35% (B).

To check whether SIRT3 knockdown was functional, the acetylation of one of its targets, MnSOD, was determined (Figure 1C). As it can be seen, when siRNA against SIRT3 was added, the acetylation of MnSOD was higher, so there was a decrease in SIRT3 activity.

*SIRT3 silencing reduces cell viability and increases the effect of cytotoxic treatment*

A cell viability assay was performed to evaluate the effect of SIRT3 silencing alone or in combination with cytotoxic treatments on cell growth. As shown in Figure 2A, SIRT3 knockdown decreased cell viability around 20% in MCF-7 cell line. TAM and CDDP reduced cell growth to 57% and 47% of control values, respectively, and when combined with SIRT3 silencing their cytotoxic effect was enhanced, further reducing viability (15% and 11% more than TAM and CDDP alone, respectively).

Accordingly, SIRT3 knockdown also affected the ability of cancer cells to form viable colonies,as was assessed by the clonogenic assay. Figure 2B shows that TAM treatment reduced colony formation by 37%, and when in combination with the siRNA against SIRT3, it decreased clonogenicity by 51%. The fewer colonies were observed in CDDP-treated cells (reduction of 69%), especially when in combination with SIRT3 silencing (reduction of 86%).

*ROS production is significantly increased in SIRT3 knockdown cells*

Since SIRT3 plays a key role regulating oxidative stress, ROS production was analyzed. Figure 2C shows that ROS production was triggered after TAM (141%) and CDDP (242%) treatments. SIRT3 knockdown significantly raised ROS production by 196%, and this effect was even greater when combined with TAM (356%) and CDDP (496%) treatments.

*Autophagy and apoptosis are enhanced with SIRT3 silencing*

SIRT3 knockdown caused a 47% increment in the formation of autophagic vacuoles, measured as MDC fluorescence, as shown in Figure 3A. Cytotoxic treatments also triggered a

rise in autophagy (268% TAM and 220% CDDP), and especially the TAM treatment showed a greater increase when combined with SIRT3 silencing (+115% compared to TAM treatment alone). Additionally, Figure 3B shows that LC3-II/LC3-I ratio (microtubule-associated protein light chain 3, a marker for the autophagy process) was increased with SIRT3 silencing and cytotoxic treatments. As can be seen with the MDC fluorescent probe, the highest values were triggered by TAM treatment alone (451%) and by the combination of TAM and siRNA against SIRT3 (583%).

Programmed cell death was also studied through the analysis of different apoptosis markers. Figure 3D shows that both TAM and CDDP increased the annexin V fluorescence by 39% and 69%, respectively. Poly (ADP-ribose) polymerase (PARP) cleavage was also higher with both treatments, as shown in Figure 3E. SIRT3 silencing alone slightly triggered apoptosis, increasing by 23% the annexin V fluorescence and by 17% the ratio cleaved PARP/PARP. However, when SIRT3 siRNA was combined with cytotoxic treatments, the effect was magnified, especially with the CDDP treatment, which increased annexin V fluorescence by 187% and PARP cleavage by 120%, compared to control values. Representative bands of Western Blot of LC3 and PARP are shown in Figure 3C and 3F, respectively.

*Mitochondrial biogenesis and antioxidant enzymes are negatively affected by SIRT3 knockdown*

Protein levels of PGC1-α, the main regulator of mitochondrial biogenesis, were analyzed. SIRT3 silencing diminished the levels of PGC1-α by 12%, as seen in Figure 4A. Cytotoxic treatments also reduced levels of this protein by around 24%, and when combined with SIRT3 knockdown, PGC1- α levels were further diminished.

TFAM, which is transcriptionally controlled by PGC-1α and regulates mitochondrial transcription and replication, was also reduced by around 27% with SIRT3 silencing. In this case, CDDP and TAM treatments alone did not affect TFAM protein levels, although when combined with siRNA against SIRT3, TFAM levels were diminished, as seen in Figure 4B.

Finally, protein levels of antioxidant enzymes that can be deacetylated by SIRT3 were also analyzed. Figure 4C shows that MnSOD, the main superoxide scavenger in mitochondria, was reduced by 20% with SIRT3 silencing. On the other hand, $IDH_2$, which regenerates NADPH to maintain the glutathione system, is also diminished by SIRT3 knockdown. As seen in Figure 4D, SIRT3 silencing diminished the levels of $IDH_2$ by 50%. Interestingly, CDDP treatment raised

levels of $IDH_2$ by 62%, although when combined with SIRT3 silencing, $IDH_2$ returned to control levels. Representative bands of these western blots are shown in Figure 4E.

*Higher expression of SIRT3 is related to a poorer prognosis in grade 3 breast cancer patients*

Figure 5A shows the Kaplan-Meier plots representing the overall survival of patients diagnosed with grade 3 ER positive breast cancer expressing high or low levels of SIRT3. Overall survival is significantly lower in those patients with higher expression of SIRT3 (P=0.018). On the other hand, no differences are observed in terms of overall survival when ER-negative breast cancer patients are considered (Figure 5B).

*SIRT3 silencing affects T47D breast cancer cells in a similar manner*

In order to confirm the results observed in MCF-7 cells, some key experiments were conducted with another breast cancer cell line, T47D. In T47D cells, 35% of SIRT3 silencing was achieved with the specific siRNA (Figure 1B).

First, the cell viability assay (Figure 6A) showed that T47D cells are more resistant to cytotoxic treatments than MCF-7. SIRT3 silencing reduced viability by 11% and improved the effectiveness of TAM and CDDP, causing around 10% and 5% more loss of viability, respectively.

ROS production was also affected in T47D cell line, although more subtly in comparison to MCF-7. As shown in Figure 6B, cells presented higher ROS production with SIRT3 knockdown (increased by 21%), as well as with cytotoxic treatments (+59% TAM and+31% CDDP). As expected, combining SIRT3 silencing with TAM or CDDP treatment further enhanced ROS production, resulting in a 40% and 23% increase, respectively.

Figure 6C shows that SIRT3 silencing also increased formation of autophagic vacuoles by 30%. As seen in MCF-7 cells, TAM treatment caused a significant increase in autophagy, especially in combination with SIRT3 knockdown (292% and 373% of control values, respectively). CDDP treatment also increased vacuole formation by 70% and by 94% with SIRT3 silencing.

Finally, Figure 6D shows that apoptosis increased by SIRT3 silencing (increased by 22%) and by cytotoxic treatments (TAM +48% and CDDP +55%), although there were no significant changes when combining treatments and siRNA, in comparison to the TAM or CDDP treatment alone.

## DISCUSSION

In this study, we have shown that SIRT3 silencing results in a lower viability for breast cancer cell lines MCF-7 and T47D, which was accompanied by the induction of apoptosis and autophagy. Furthermore, this lower viability occurred with an increase in ROS production, which could be explained by the reduction in protein levels related to mitochondrial biogenesis (PGC-1α and TFAM), and in enzymes such as MnSOD and $IDH_2$, which take part in ROS scavenging. Combination of SIRT3 silencing with TAM or CDDP treatments produced an increase in the efficacy of these cytotoxic compounds that was accompanied by an increase in ROS production, showing a synergic effect.

In both MCF7 and T47D cell lines, knockdown of SIRT3 diminished cell viability by about 15% as well as their ability to form viable colonies. These results are in agreement with other studies showing that SIRT3 promotes cell survival in normal cells and protects them from cell death by maintaining mitochondrial homeostasis and enhancing antioxidant systems (Alhazzazi et al., 2013; Finley and Haigis, 2012; Weir et al., 2013). Furthermore, expression of SIRT3 has been linked to a higher and more aggressive growth of several types of cancer (Alhazzazi et al., 2011; Ashraf et al., 2006; Cui et al., 2015). In this regard, bioinformatics tools show that SIRT3 expression is related to breast cancer patient prognosis. In this case, higher expression of SIRT3 in ER-positive grade 3 breast cancer patients corresponded to a poorer prognosis with a lower overall survival, as seen by other studies and in other types of cancer (He et al., 2014; Liu et al., 2014; Zhang et al., 2013).

Nevertheless, other studies show the opposite: decreased expression of SIRT3 is associated with poorer prognosis in different types of cancer (Desouki et al., 2014; Liu et al., 2014). It is important to note that we have only considered patients in an advanced stage of breast cancer (grade 3) for the determination of the effect on overall survival rate. When all grades are taken into account, SIRT3 expression is conversely correlated to survival and relapse-free survival. These contradictory results could be explained due to the dual role that SIRT3 plays in cancer, as was observed with other proteins that regulate oxidative stress (Pons et al., 2015a). In healthy tissue and in the initial stages of cancer, an increase in ROS levels induces cell proliferation (Laurent et al., 2005; Roca et al., 2014; Valle and Roca, 2012), thus a reduction in SIRT3 levels allows an increase in oxidative stress and cell transformation. On the other hand, in the advanced stages of cancer, ROS rises to excessive levels that are incompatible with cell survival and lead to apoptosis (Laurent et al., 2005; Roca et al., 2014; Valle and Roca, 2012). In

this situation, a lower expression of SIRT3 could contribute to an increase in oxidative stress and induce cell death (Papa and Germain, 2014).

Consequently, SIRT3 can contribute to cell survival by balancing ROS levels in order to promote cell proliferation and transformation, avoiding the activation of apoptosis pathways (Alhazzazi et al., 2013; Papa and Germain, 2014). The reduced viability observed when SIRT3 is silenced may be due to an increment of apoptosis, probably triggered by the increase in ROS production. Apoptosis induction by high levels of ROS has been described before (Alhazzazi et al., 2013; Pons et al., 2015a; Roca et al., 2014). In this regard, our results show that with SIRT3 knockdown ROS production is enhanced to excessive levels that are incompatible with cellular viability, which thus triggers the apoptosis process.

Both mitochondrial turnover (biogenesis-mitophagy) as well as the activity of antioxidant enzymes are regulated by SIRT3, which may explain the higher ROS production observed when SIRT3 is silenced. SIRT3 deacetylates and activates key mitochondrial proteins such as the subunits of the OXPHOS complexes, MnSOD or $IDH_2$, leading to a reduction of oxidative stress (Bause and Haigis, 2013; Finley and Haigis, 2012; Sack and Finkel, 2012). MnSOD is one of the main ROS scavengers in mitochondria and its deacetylation enhances its superoxide removal activity (Chen et al., 2011; Ozden et al., 2011; Zhu et al., 2014). On the other hand, $IDH_2$, which is more active when deacetylated,generates NADPH, essential in maintaining other cellular antioxidant defenses (Weir et al., 2013).

In addition to these action mechanisms, we also observed that SIRT3 knockdown reduced the protein levels of PGC1-α, TFAM, MnSOD and $IDH_2$. These results are in agreement with previous studies that have described SIRT3 to deacetylate and promote the nuclear localization of the transcription factor FOXO3a, which controls the expression of antioxidant enzymes such as MnSOD, catalase, and $IDH_2$, and the expression of proteins which regulate mitochondrial turnover, such as TFAM and PGC-1α (Bause and Haigis, 2013; Tseng et al., 2013; Weir et al., 2013). Therefore, SIRT3 silencing could produce a less functional mitochondria pool, due to the reduction in proteins that regulate mitochondrial biogenesis and the reduction in the antioxidant enzymes that maintain mitochondrial integrity, which would in turn result in higher levels of oxidative stress.

SIRT3 silencing also enhanced the formation of autophagic vacuoles. Autophagy is a highly conserved process that mediates the degradation of damaged components or organelles, participating in their turnover and in cellular homeostasis under normal conditions (Cook et al., 2011; Poillet-Perez et al., 2015). Autophagy has been linked to cell survival, as it is considered

to be a cell protection mechanism to recover energy from unnecessary or damaged subcellular components (Cook et al., 2011; Zarzynska, 2014). However, if high levels of autophagy persist due to severe damage, autophagic cell death or programmed cell death-2 may occur (Bellot et al., 2013; Scherz-Shouval and Elazar, 2007). Autophagy is usually limited by the mTOR signaling pathway, which is inhibited under certain stresses (Scherz-Shouval and Elazar, 2011). ROS levels are known to induce autophagy by activating AMPK signaling, which inhibits mTOR (Li et al., 2012; Poillet-Perez et al., 2015; Scherz-Shouval and Elazar, 2011). Moreover, severely damaged mitochondria may directly induce autophagy by the PARKIN/PINK pathway in order to reduce the main source of ROS production (Poillet-Perez et al., 2015).

Taken together, these results are in agreement with the crucial role that SIRT3 plays as a fidelity protein in mitochondria, maintaining the integrity and proper function of these organelles, as well as contributing to cell survival and limiting ROS production (Kim et al., 2010; Park et al., 2011).Moreover, several studies have shown that SIRT3 is also relevant in an in vivo context. Different xenograft studies have been performed to show that SIRT3 knockdown inhibits cell proliferation and decreases the tumour growth of melanoma, gastric cancer and renal cell carcinoma (Choi et al., 2016; Cui et al., 2015; George et al., 2015).

The cytotoxic effect of CDDP is based in its interaction and binding to DNA, which creates adducts that difficult DNA replication and lead to activation of apoptosis (Kelland, 2007; Siddik, 2003). Moreover, some studies show that CDDP targets mitochondria, causing a reduction in their functionality and an important increase in ROS production (Marullo et al., 2013; Pons et al., 2015a). Thus, CDDP induces apoptosis in a ROS-dependent way (Huang et al., 2003; Marullo et al., 2013). In this regard, our results show that CDDP treatment significantly increases apoptosis, as seen by the increase in annexin fluorescence and by the higher ratio of cleaved PARP/PARP, while autophagy markers are notably less affected. CDDP also enhances ROS production in comparison to control values and also triggers autophagy, probably because of the higher ROS production and the severely damaged mitochondria. Moreover, when SIRT3 is silenced, ROS production is further increased, showing an important synergic effect (increasing 5-fold), while apoptosis is highly enhanced compared to CDDP treatment or SIRT3 silencing alone. Similar results were observed in T47D cell line, although these cells are more resistant to cytotoxic treatments at the concentration used in this study, as has been previously reported by our group (D. Pons et al., 2015b).

On the other hand, TAM is commonly used to treat ER-positive breast cancer patients, since this compound is an ER-α antagonist. However, TAM cytotoxicity is also related to an increase

in ROS production (D. Pons et al., 2015b). In this regard, our results showed that TAM triggers ROS production and, differently to CDDP, induces autophagy. Thus, TAM may induce cell death through a different mechanism from that of CDDP, as previously described by our group (D. Pons et al., 2015a, 2015b). These results are in agreement with some studies that have shown that TAM may activate AMPK, and thus induce the formation of autophagic vacuoles (Zarzynska, 2014). When TAM treatment is combined with SIRT3 silencing, both ROS production and autophagy are increased. A possible explanation is that since the AMPK pathway is activated by both TAM treatment and ROS levels, and that mitochondria are damaged by SIRT3 silencing, autophagy may be activated through several pathways. As mentioned before, the results in T47D are similar, although this cell line is less responsive to changes in oxidative stress (Pons et al., 2015b).

In conclusion, SIRT3 knockdown could be an adjuvant treatment for breast cancer, improving the effectiveness of chemotherapy and hormonal therapy by enhancing their different action mechanisms. Moreover, our results show the crucial role of SIRT3 in regulation of mitochondria homeostasis and oxidative stress.

**Conflict of interest**

The authors report no conflicts of interest. The authors alone are responsible for the content and writing of the paper.

**Acknowledgments**

This work was supported by grants from Fondo de Investigaciones Sanitarias of Instituto de Salud Carlos III (PI12/01827 and PI14/01434) of the Spanish Government confinanced by FEDER-Unión Europea ("Una manera de hacer Europa") and funds from Comunitat Autònoma de les Illes Balears and FEDER (31/2011 and AAEE22/2014). D.G. Pons was funded by a grant from Comunidad Autónoma de las Islas Baleares cofinanced by Fondo Social Europeo, and M. Torrens-Mas by an FPU grant from Ministerio de Educación, Cultura y Deporte of Spanish Government.

## References


Alhazzazi, T.Y., Kamarajan, P., Joo, N., Huang, J.-Y., Verdin, E., D'Silva, N.J., Kapila, Y.L., 2011. Sirtuin-3 (SIRT3), a novel potential therapeutic target for oral cancer. Cancer 117, 1670–8.

Alhazzazi, T.Y., Kamarajan, P., Verdin, E., Kapila, Y.L., 2013. Sirtuin-3 (SIRT3) and the Hallmarks of Cancer. Genes Cancer 4, 164–71.

Ashraf, N., Zino, S., Macintyre, a, Kingsmore, D., Payne, a P., George, W.D., Shiels, P.G., 2006. Altered sirtuin expression is associated with node-positive breast cancer. Br. J. Cancer 95, 1056–1061.

Bause, A.S., Haigis, M.C., 2013. SIRT3 regulation of mitochondrial oxidative stress. Exp. Gerontol. 48, 634–639.

Bellot, G.L., Liu, D., Pervaiz, S., 2013. ROS, autophagy, mitochondria and cancer: Ras, the hidden master? Mitochondrion 13, 155–162.

Chen, J.-Q., Brown, T.R., Yager, J.D., 2008. Mechanisms of hormone carcinogenesis: evolution of views, role of mitochondria. Adv. Exp. Med. Biol. 630, 1–18.

Chen, Y., Fu, L.L., Wen, X., Wang, X.Y., Liu, J., Cheng, Y., Huang, J., 2014. Sirtuin-3 (SIRT3), a therapeutic target with oncogenic and tumor-suppressive function in cancer. Cell Death Dis. 5, e1047.

Chen, Y., Zhang, J., Lin, Y., Lei, Q., Guan, K.-L., Zhao, S., Xiong, Y., 2011. Tumour suppressor SIRT3 deacetylates and activates manganese superoxide dismutase to scavenge ROS. EMBO Rep. 12, 534–41.

Choi, J., Koh, E., Lee, Y.S., Lee, H.-W., Kang, H.G., Yoon, Y.E., Han, W.K., Choi, K.H., Kim, K.-S., 2016. Mitochondrial Sirt3 supports cell proliferation by regulating glutamine-dependent oxidation in renal cell carcinoma. Biochem. Biophys. Res. Commun. 474, 547–553.

Cook, K.L., Shajahan, A.N., Clarke, R., 2011. Autophagy and endocrine resistance in breast cancer. Expert Rev. Anticancer Ther. 11, 1283–1294.

Cui, Y., Qin, L., Wu, J., Qu, X., Hou, C., Sun, W., Li, S., Vaughan, A.T.M., Li, J.J., Liu, J., 2015. SIRT3 Enhances Glycolysis and Proliferation in SIRT3-Expressing Gastric Cancer Cells. PLoS One 10, e0129834.

Dando, I., Fiorini, C., Pozza, E.D., Padroni, C., Costanzo, C., Palmieri, M., Donadelli, M., 2013. UCP2 inhibition triggers ROS-dependent nuclear translocation of GAPDH and autophagic cell death in pancreatic adenocarcinoma cells. Biochim. Biophys. Acta - Mol. Cell Res. 1833, 672–679.

Desouki, M.M., Doubinskaia, I., Gius, D., Abdulkadir, S.A., 2014. Decreased mitochondrial SIRT3 expression is a potential molecular biomarker associated with poor outcome in breast cancer. Hum. Pathol. 45, 1071–7.

Ferlay, J., Soerjomataram, I., Ervik, M., Dikshit, R., Eser, S., Mathers, C., Rebelo, M., Parkin, D., Forman, D., Bray, F., 2013. GLOBOCAN 2012 v1.0, Cancer Incidence and Mortality Worldwide: IARC CancerBase No. 11. Lyon, Fr. Int. Agency Res. Cancer.

Finley, L.W.S., Haigis, M.C., 2012. Metabolic regulation by SIRT3: Implications for tumorigenesis. Trends Mol. Med. 18, 516–523.

George, J., Nihal, M., Singh, C.K., Zhong, W., Liu, X., Ahmad, N., 2015. Pro-Proliferative Function of Mitochondrial Sirtuin Deacetylase SIRT3 in Human Melanoma. J. Invest. Dermatol. 1–10.

Gyorffy, B., Lanczky, A., Eklund, A., Denkert, C., Budczies, J., Li, Q., Szallasi, Z., 2010. An online survival analysis tool to rapidly assess the effect of 22,277 genes on breast cancer prognosis using microarray data of 1809 patients. Breast Cancer Res Treat. 123, 725–31.

He, S., He, C., Yuan, H., Xiong, S., Xiao, Z., Chen, L., 2014. The SIRT 3 expression profile is associated with pathological and clinical outcomes in human breast cancer patients. Cell. Physiol. Biochem. 34, 2061–9.

Huang, H.-L., Fang, L.-W., Lu, S.-P., Chou, C.-K., Luh, T.-Y., Lai, M.-Z., 2003. DNA-damaging reagents induce apoptosis through reactive oxygen species-dependent Fas aggregation. Oncogene 22, 8168–8177.

Kelland, L., 2007. The resurgence of platinum-based cancer chemotherapy. Nat. Rev. Cancer 7, 573–584.

Kim, H.S., Patel, K., Muldoon-Jacobs, K., Bisht, K.S., Aykin-Burns, N., Pennington, J.D., van der Meer, R., Nguyen, P., Savage, J., Owens, K.M., Vassilopoulos, A., Ozden, O., Park, S.H., Singh, K.K., Abdulkadir, S.A., Spitz, D.R., Deng, C.X., Gius, D., 2010. SIRT3 Is a Mitochondria-Localized Tumor Suppressor Required for Maintenance of Mitochondrial Integrity and Metabolism during Stress. Cancer Cell 17, 41–52.

Laurent, A., Nicco, C., Chéreau, C., Goulvestre, C., Alexandre, J., Alves, A., Lévy, E., Goldwasser, F., Panis, Y., Soubrane, O., Weill, B., Batteux, F., 2005. Controlling tumor growth by modulating endogenous production of reactive oxygen species. Cancer Res. 65, 948–56.

Li, L., Ishdorj, G., Gibson, S.B., 2012. Reactive oxygen species regulation of autophagy in cancer: Implications for cancer treatment. Free Radic. Biol. Med. 53, 1399–1410.

Liu, C., Huang, Z., Jiang, H., Shi, F., 2014. The Sirtuin 3 Expression Profile Is Associated with Pathological and Clinical Outcomes in Colon Cancer Patients. Biomed Res. Int. 2014:87126.

Marullo, R., Werner, E., Degtyareva, N., Moore, B., Altavilla, G., Ramalingam, S.S., Doetsch, P.W., 2013. Cisplatin Induces a Mitochondrial-ROS Response That Contributes to Cytotoxicity Depending on Mitochondrial Redox Status and Bioenergetic Functions. PLoS One 8, e81162.

Nadal-Serrano, M., Sastre-Serra, J., Pons, D.G., Miró, A.M., Oliver, J., Roca, P., 2012. The ERalpha/ERbeta ratio determines oxidative stress in breast cancer cell lines in response to 17beta-estradiol. J. Cell. Biochem. 113, 3178–85.

Ozden, O., Park, S.H., Kim, H.S., Jiang, H., Coleman, M.C., Spitz, D.R., Gius, D., 2011. Acetylation of MnSOD directs enzymatic activity responding to cellular nutrient status or oxidative stress. Aging (Albany. NY). 3, 102–107.

Papa, L., Germain, D., 2014. SirT3 Regulates the Mitochondrial Unfolded Protein Response 34, 699–710.

Park, S.-H., Ozden, O., Jiang, H., Cha, Y.I., Pennington, J.D., Aykin-Burns, N., Spitz, D.R., Gius, D., Kim, H.-S., 2011. Sirt3, mitochondrial ROS, ageing, and carcinogenesis. Int. J. Mol. Sci. 12, 6226–39.

Poillet-Perez, L., Despouy, G., Delage-Mourroux, R., Boyer-Guittaut, M., 2015. Interplay between ROS and autophagy in cancer cells, from tumor initiation to cancer therapy. Redox Biol. 4, 184–192.

Pons, D., Nadal-Serrano, M., Torrens-Mas, M., Valle, A., Oliver, J., Roca, P., 2015a. UCP2 inhibition sensitizes breast cancer cells to therapeutic agents by increasing oxidative

stress. Free Radic. Biol. Med. 86, 67–77.

Pons, D., Torrens-Mas, M., Nadal-Serrano, M., Sastre-Serra, J., Roca, P., Oliver, J., 2015b. The presence of Estrogen Receptor β modulates the response of breast cancer cells to therapeutic agents. Int. J. Biochem. Cell Biol. 66, 85–94.

Razandi, M., Pedram, A., Jordan, V.C., Fuqua, S., Levin, E.R., 2013. Tamoxifen regulates cell fate through mitochondrial estrogen receptor beta in breast cancer. Oncogene 32, 3274–85.

Roca, P., Sastre-Serra, J., Nadal-Serrano, M., Pons, D.G., Blanquer-Rossello, M.D.M., Oliver, J., 2014. Phytoestrogens and Mitochondrial Biogenesis in Breast Cancer. Influence of Estrogen Receptors Ratio. Curr. Pharm. Des. 20, 5594 – 5618.

Sack, M.N., Finkel, T., 2012. Mitochondrial metabolism, sirtuins, and aging. Cold Spring Harb. Perspect. Biol. 4, a013102–.

Sainz, R.M., Lombo, F., Mayo, J.C., 2012. Radical decisions in cancer: redox control of cell growth and death. Cancers (Basel). 4, 442–74.

Sastre-Serra, J., Nadal-Serrano, M., Pons, D.G., Valle, A., Oliver, J., Roca, P., 2012. The effects of 17beta-estradiol on mitochondrial biogenesis and function in breast cancer cell lines are dependent on the ERalpha/ERbeta ratio. Cell Physiol Biochem 29, 261–268.

Scherz-Shouval, R., Elazar, Z., 2011. Regulation of autophagy by ROS: physiology and pathology. Trends Biochem. Sci. 36, 30–38.

Scherz-Shouval, R., Elazar, Z., 2007. ROS, mitochondria and the regulation of autophagy. Trends Cell Biol. 17, 422–427.

Siddik, Z.H., 2003. Cisplatin: mode of cytotoxic action and molecular basis of resistance. Oncogene 22, 7265–7279.

Tseng, A.H.H., Shieh, S.S., Wang, D.L., 2013. SIRT3 deacetylates FOXO3 to protect mitochondria against oxidative damage. Free Radic. Biol. Med. 63, 222–234.

Valle, A., Roca, P., 2012. Mitochondria at the Crossroads of Cancer and Oxidative Stress, Handbook on Oxidative Stress. New Research. Nova Science Publishers, Inc.

Wei, L., Zhou, Y., Dai, Q., Qiao, C., Zhao, L., Hui, H., Lu, N., Guo, Q.-L., 2013. Oroxylin A induces dissociation of hexokinase II from the mitochondria and inhibits glycolysis by SIRT3-mediated deacetylation of cyclophilin D in breast carcinoma. Cell Death Dis. 4, e601.

Weir, H.J.M., Lane, J.D., Balthasar, N., 2013. SIRT3: A Central Regulator of Mitochondrial Adaptation in Health and Disease. Genes Cancer 4, 118–24.

Youlden, D.R., Cramb, S.M., Dunn, N.A.M., Muller, J.M., Pyke, C.M., Baade, P.D., 2012. The descriptive epidemiology of female breast cancer: an international comparison of screening, incidence, survival and mortality. Cancer Epidemiol. 36, 237–48.

Zarzynska, J., 2014. The importance of Autophagy Regulation in Breast Cancer Development and Treatment. Biomed Res. Int. 2014.

Zhang, L., Ren, X., Cheng, Y., Huber-Keener, K., Liu, X., Zhang, Y., Yuan, Y.S., Yang, J.W., Liu, C.G., Yang, J.M., 2013. Identification of Sirtuin 3, a mitochondrial protein deacetylase, as a new contributor to tamoxifen resistance in breast cancer cells. Biochem. Pharmacol. 86, 726–733.

Zhu, Y., Yan, Y., Principe, D., 2014. SIRT3 and SIRT4 are mitochondrial tumor suppressor proteins that connect mitochondrial metabolism and carcinogenesis. Cancer & Metabolism 2014, 2:15.

**FIGURE LEGENDS**

Figure 1. SIRT3 Western Blots. (A) Representative bands of SIRT3 (28 kDa) Western Blot for the MCF-7 cell line after siRNA transfection for 72 hours. GAPDH was used as housekeeping. (B) Representative bands of SIRT3 Western Blot for T47D cell line after siRNA transfection. GAPDH was used as housekeeping. (C) Acetylation of MnSOD. Representative bands of the acetylation of MnSOD, target of SIRT3, are shown for MCF-7 cell line after siRNA transfection for 72 hours. The control for these IP experiments is normalized to rabbit IgG.

Figure 2. MCF-7 cell viability and colony formation diminished after SIRT3 siRNA and cytotoxic treatments, while ROS production was significantly increased. (A) Cell proliferation was assessed by crystal violet assay. (B) Clonogenic assay was performed as described under Materials and Methods section. (C) ROS production was assessed fluorimetrically by Amplex Red® method. All determinations were made after siRNA transfection and treatment with 10 µM cisplatin or 10 µM tamoxifen for 48 hours. Values are expressed as means ± SEM (n=6) and normalized as percentage of the control value. Control cells are shown in white, and cells transfected with SIRT3 siRNA in black. ANOVA analysis was carried out where: S indicates a siRNA effect, C cisplatin effect, T tamoxifen effect, and CxS or TxS indicates a combinatory effect of the respective cytotoxic compound and siRNA. A Student's t test ($P<0.05$) was performed when combinatory effects were observed where: * indicates a significant difference between vehicle and siRNA-treated cells; ° between control and cytotoxic treatment.

Figure 3. Autophagy and apoptosis were enhanced with SIRT3 siRNA transfection and cytotoxic treatments. (A) Autophagic vacuole formation was measured fluorimetrically using the monodansylcadaverine probe. (B) LC3-II/LC3-I protein expression was measured by Western blot analysis. (C) Representative bands of LC3-II (14 kDa) and LC3-I (16 kDa) Western Blot. GAPDH was used as a housekeeping protein. (D) Apoptosis was measured fluorimetrically using the annexin-V probe. (E) Cleaved PARP/PARP ratio was measured by Western blot. (F) Representative bands of PARP (116 kDa) and cleaved PARP (89 kDa) Western Blot. GAPDH was used as a housekeeping protein. All determinations were performed after siRNA transfection and treatment with 10 µM cisplatin or 10 µM tamoxifen for 48 hours. Values are expressed as means ± SEM (n=6) and normalized as percentage of the control value. Control cells are shown in white, and cells transfected with SIRT3 siRNA are shown in black. ANOVA analysis was carried out where: S indicates siRNA effect, C cisplatin effect, T tamoxifen effect, and CxS or TxS indicates a combinatory effect of the respective cytotoxic compound and siRNA. A Student's t test ($P<0.05$) was performed when combinatory effects were observed where: *

indicates a significant difference between vehicle and siRNA-treated cells; ° between control and cytotoxic treatment.

Figure 4. PGC-1α,T FAM, MnSOD and $IDH_2$ protein levels after siRNA transfection and cytotoxic treatments. Western Blots of (A) PGC-1α; (B) TFAM; (C) MnSOD; and (D) $IDH_2$. Representative Western Blot analysis bands for MnSOD, $IDH_2$, PGC-1α and TFAM. GAPDH was used as a housekeeping protein. All determinations were performed after siRNA transfection and treatment with 10 μM cisplatin or 10 μM tamoxifen for 48 hours. Values are expressed as means ± SEM (n=6) and normalized as percentage of the control value. Control cells are shown in white, and cells transfected with SIRT3 siRNA in black. ANOVA analysis was carried out where: S indicates a siRNA effect, C cisplatin effect, and T tamoxifen effect.

Figure 5. Kaplan-Meier survival curves show that high SIRT3 expression corresponds to a lower overall survival for ER-positive grade 3 breast cancer patients. (A) Kaplan-Meier plot for ER+ 3 grade breast cancer patients. (B) Kaplan-Meier plot for ER- 3 grade breast cancer patients. Kaplan–Meier plots were made using the online (www.kmplot.com) Kaplan–Meier plotter dataset.

Figure 6. Cell viability, ROS production, autophagy and apoptosis in T47D after siRNA transfection and cytotoxic treatments. (A) Cell viability was assessed by crystal violet assay. (B) ROS production was assessed fluorimetrically with Amplex Red reagent. (C) Autophagic vacuole formation was measured fluorimetrically using the monodansylcadaverine probe. (D) Apoptosis was measured fluorimetrically using the annexin-V probe. All determinations were performed after siRNA transfection and treatment with 10 μM cisplatin or 10 μM tamoxifen for 48 hours. Values are expressed as means ± SEM (n=6) and normalized as percentage of the control value. Control cells are shown in white, and cells transfected with SIRT3 siRNA in black. ANOVA analysis was performed where: S indicates a siRNA effect, C (cisplatin effect), T (tamoxifen effect), and CxS or TxS indicates a combinatory effect of the respective cytotoxic compound and siRNA. A Student's t test ($P<0.05$) was performed when combinatory effects were observed where: * indicates a significant difference between vehicle and siRNA-treated cells; and ° between control and cytotoxic treatment.

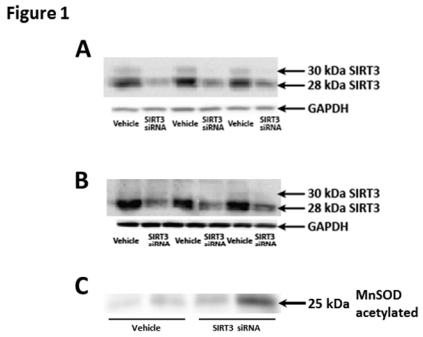


Figure 1. SIRT3 Western Blots. (A) Representative bands of SIRT3 (28 kDa) Western Blot for the MCF-7 cell line after siRNA transfection for 72 hours. GAPDH was used as housekeeping. (B) Representative bands of SIRT3 Western Blot for T47D cell line after siRNA transfection. GAPDH was used as housekeeping. (C) Acetylation of MnSOD. Representative bands of the acetylation of MnSOD, target of SIRT3, are shown for MCF-7 cell line after siRNA transfection for 72 hours. The control for these IP experiments is normalized to rabbit IgG.

366x275mm (96 x 96 DPI)

Figure 2

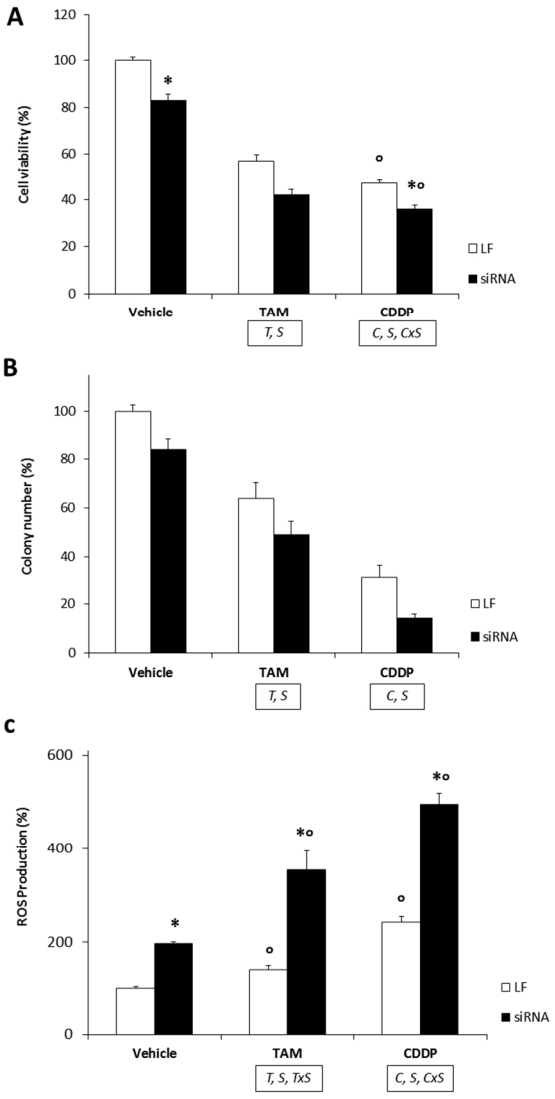


Figure 2. MCF-7 cell viability and colony formation diminished after SIRT3 siRNA and cytotoxic treatments, while ROS production was significantly increased. (A) Cell proliferation was assessed by crystal violet assay. (B) Clonogenic assay was performed as described under Materials and Methods section. (C) ROS production was assessed fluorimetrically by Amplex Red® method. All determinations were made after siRNA transfection and treatment with 10 μM cisplatin or 10 μM tamoxifen for 48 hours. Values are expressed as means ± SEM (n=6) and normalized as percentage of the control value. Control cells are shown in white, and cells transfected with SIRT3 siRNA in black. ANOVA analysis was carried out where: S indicates a siRNA effect, C cisplatin effect, T tamoxifen effect, and CxS or TxS indicates a combinatory effect of the respective cytotoxic compound and siRNA. A Student's t test ($P<0.05$) was performed when combinatory effects were observed where: * indicates a significant difference between vehicle and siRNA-treated cells; ° between control and cytotoxic treatment.

255x405mm (96 x 96 DPI)

**Figure 3**

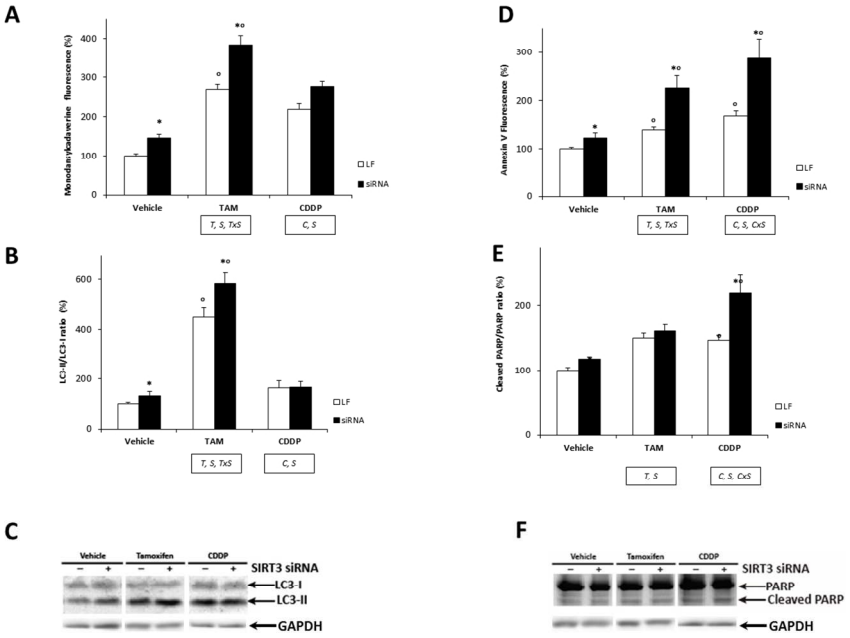


Figure 3. Autophagy and apoptosis were enhanced with SIRT3 siRNA transfection and cytotoxic treatments. (A) Autophagic vacuole formation was measured fluorimetrically using the monodansylcadaverine probe. (B) LC3-II/LC3-I protein expression was measured by Western blot analysis. (C) Representative bands of LC3-II (14 kDa) and LC3-I (16 kDa) Western Blot. GAPDH was used as a housekeeping protein. (D) Apoptosis was measured fluorimetrically using the annexin-V probe. (E) Cleaved PARP/PARP ratio was measured by Western blot. (F) Representative bands of PARP (116 kDa) and cleaved PARP (89 kDa) Western Blot. GAPDH was used as a housekeeping protein. All determinations were performed after siRNA transfection and treatment with 10 μM cisplatin or 10 μM tamoxifen for 48 hours. Values are expressed as means ± SEM (n=6) and normalized as percentage of the control value. Control cells are shown in white, and cells transfected with SIRT3 siRNA are shown in black. ANOVA analysis was carried out where: S indicates siRNA effect, C cisplatin effect, T tamoxifen effect, and CxS or TxS indicates a combinatory effect of the respective cytotoxic compound and siRNA. A Student's t test ($P<0.05$) was performed when combinatory effects were observed where: * indicates a significant difference between vehicle and siRNA-treated cells; ° between control and cytotoxic treatment.

366x275mm (96 x 96 DPI)

**Figure 4**

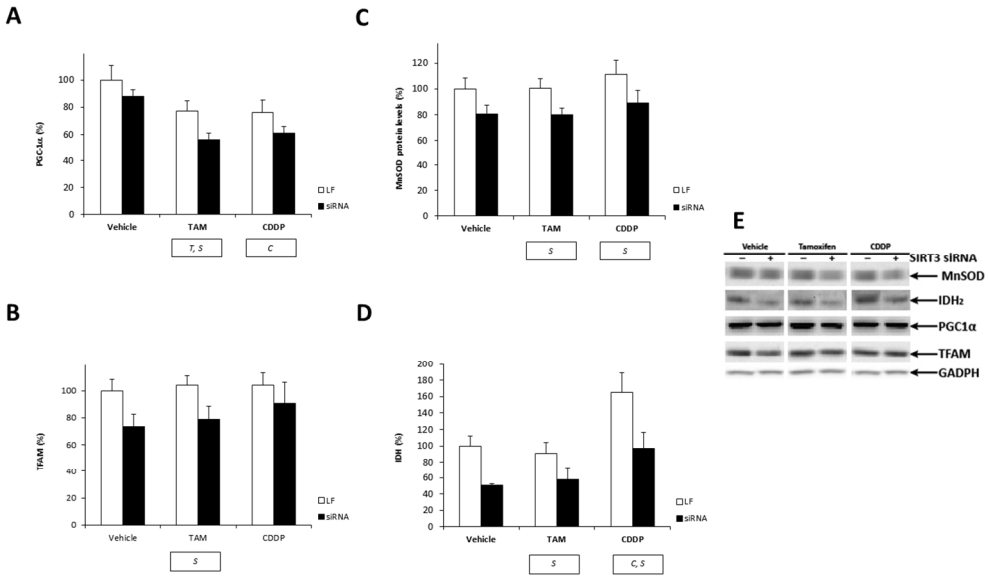


Figure 4. PGC-1α,T FAM, MnSOD and IDH2 protein levels after siRNA transfection and cytotoxic treatments. Western Blots of (A) PGC-1α; (B) TFAM; (C) MnSOD; and (D) IDH2. (E) Representative Western Blot analysis bands for MnSOD, IDH2, PGC-1α and TFAM. GAPDH was used as a housekeeping protein. All determinations were performed after siRNA transfection and treatment with 10 μM cisplatin or 10 μM tamoxifen for 48 hours. Values are expressed as means ± SEM (n=6) and normalized as percentage of the control value. Control cells are shown in white, and cells transfected with SIRT3 siRNA in black. ANOVA analysis was carried out where: S indicates a siRNA effect, C cisplatin effect, and T tamoxifen effect.

366x275mm (96 x 96 DPI)

# Figure 5

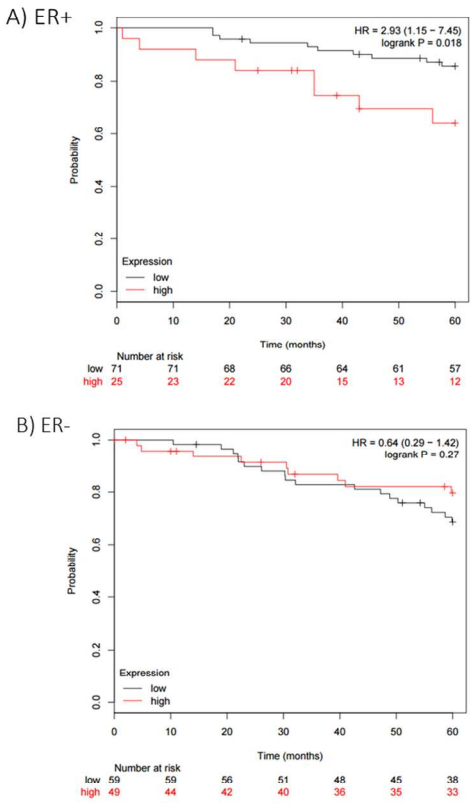


Figure 5. Kaplan-Meier survival curves show that high SIRT3 expression corresponds to a lower overall survival for ER-positive grade 3 breast cancer patients. (A) Kaplan-Meier plot for ER+ 3 grade breast cancer patients. (B) Kaplan-Meier plot for ER- 3 grade breast cancer patients. Kaplan–Meier plots were made using the online (www.kmplot.com) Kaplan–Meier plotter dataset.

300x400mm (96 x 96 DPI)

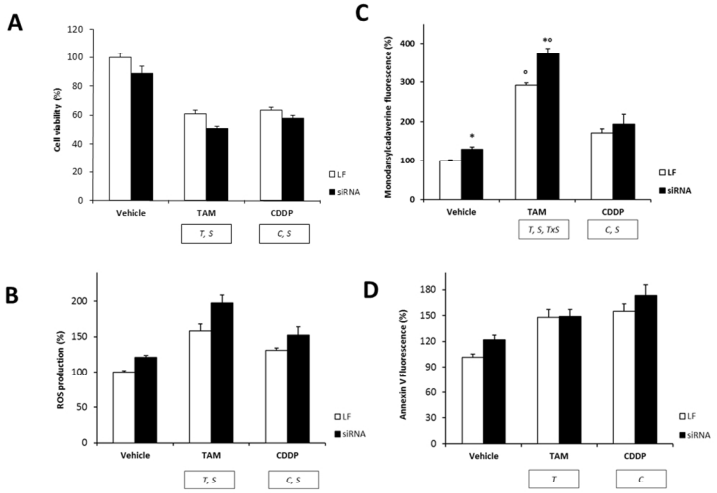


Figure 6. Cell viability, ROS production, autophagy and apoptosis in T47D after siRNA transfection and cytotoxic treatments. (A) Cell viability was assessed by crystal violet assay. (B) ROS production was assessed fluorimetrically with Amplex Red reagent. (C) Autophagic vacuole formation was measured fluorimetrically using the monodansylcadaverine probe. (D) Apoptosis was measured fluorimetrically using the annexin-V probe. All determinations were performed after siRNA transfection and treatment with 10 µM cisplatin or 10 µM tamoxifen for 48 hours. Values are expressed as means ± SEM (n=6) and normalized as percentage of the control value. Control cells are shown in white, and cells transfected with SIRT3 siRNA in black. ANOVA analysis was performed where: S indicates a siRNA effect, C (cisplatin effect), T (tamoxifen effect), and CxS or TxS indicates a combinatory effect of the respective cytotoxic compound and siRNA. A Student's t test ($P<0.05$) was performed when combinatory effects were observed where: * indicates a significant difference between vehicle and siRNA-treated cells; and ° between control and cytotoxic treatment.

366x275mm (96 x 96 DPI)